2018 IEEE-RAS 18th International Conference on Humanoid Robots (Humanoids)
Beijing, China, November 6-9, 2018

Bipedal Locomotion Up Sandy Slopes: Systematic Experiments Using Zero Moment Point Methods

Jonathan R. Gosyne[1], Christian M. Hubicki[2], Xiaobin Xiong[3], Aaron D. Ames[4] and Daniel I. Goldman[5]

***Abstract*— Bipedal robotic locomotion in granular media presents a unique set of challenges at the intersection of granular physics and robotic locomotion. In this paper, we perform a systematic experimental study in which biped robotic gaits for traversing a sandy slope are empirically designed using Zero Moment Point (ZMP) methods. We are able to implement gaits that allow our 7 degree-of-freedom planar walking robot to ascend slopes with inclines up to 10°. Firstly, we identify a given set of kinematic parameters that meet the ZMP stability criterion for uphill walking at a given angle. We then find that further relating the step lengths and center of mass heights to specific slope angles through an interpolated fit allows for significantly improved success rates when ascending a sandy slope. Our results provide increased insight into the design, sensitivity and robustness of gaits on granular material, and the kinematic changes necessary for stable locomotion on complex media.**

I. INTRODUCTION

Enabling humanoid machines to walk wherever humans can go is an ongoing robotics challenge. This challenge is especially apparent when walking on the complex and dynamic terrain present in the natural world, such as a sand dune – a sloped surface of granular material. Every footfall will sink into the non-rigid terrain exhibiting variable dynamics with respect to time and space. Additionally, an intruding foot can cause the loose material to yield, thereby slipping backward and deviating significantly from the planned walking dynamics. Further, the sand grains themselves may avalanche down the slope under pressure, creating unanticipated changes in the ground reaction forces. All of these factors can contribute to robot falls. In this paper, we experimentally investigate the control problem of robotic walking up a sandy slope by systematically adjusting the free design parameters present in established Zero Moment Point (ZMP) techniques [1, 2]. In the past, many walking robots have made use of control methods such as Hybrid Zero Dynamics (HZD) [3, 4], Zero Moment Point (ZMP) [1], and other methods of keeping the body upright [5], to ensure quasistatic or dynamic stability of the system. These methods can be then used to generate predetermined planar, or even three-dimensional paths for the biped system to follow [6]. Many of these schemes have been implemented across a variety of environments, and are typically augmented by position and acceleration feedback [1, 3, 7–15]. Methods which further employ force-based feedback can accommodate deformable terrain [16–21]. However, granular terrain poses a particular challenge given its highly nonlinear dynamics and ability to both act like a solid and flow in a fluid-like regime (yielding or avalanching) during foot contact [22, 23]. As a consequence,

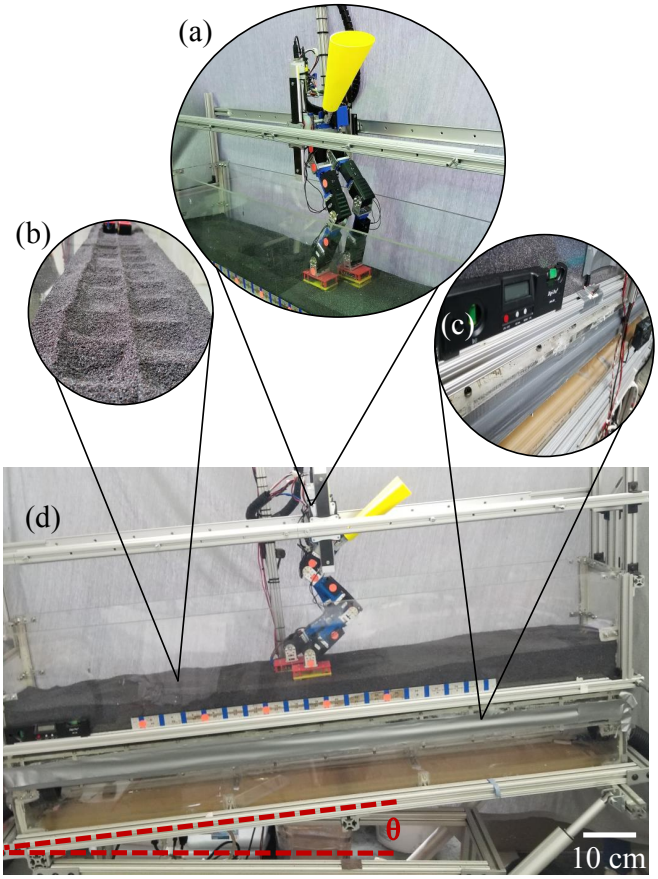

Fig. 1: (a) A picture of the 7 degree of freedom planar biped robotic walker used during the experimental trials. (b) Staircase tracks made in the poppyseed bed used, reflecting the type of gait design methods used. Poppy seeds were used to simulate coarse sand in order to avoid excess wear on the biped walker. (c) Microcontroller and leveling system for the testbed that controls slope angle. (d) The robot constrained to the sagittal plane during an experimental trial on the bed.

*This work is supported by NASA NRI Grant RG053, NSF AITF Grant 4106F91 and Army Grant 4106G16

[1]Jonathan R. Gosyne is with the School of Mechanical Engineering, Georgia Institute of Technology, Atlanta GA 30332 jonathan.gosyne@gatech.edu

[2]Christian M. Hubicki is with the Department of Mechanical Engineering, Florida State University, Tallahassee FL 32310 hubicki@gatech.edu

[3]Xiaobin Xiong is with the Department of Mechanical and Civil Engineering, California Institute of Technology, Pasadena, CA 91125 xxiong@caltech.edu

[4]Aaron D. Ames is with the Department of Mechanical and Civil Engineering, California Institute of Technology and Control and Dynamical Systems, , Pasadena, CA 91125 ames@caltech.edu

[5]Daniel I. Goldman is with the School of Physics, Georgia Institute of Technology, Atlanta GA 30332 daniel.goldman@physics.gatech.edu

if the terrain transitions from a solid-like material to flowing material as a result of the foot fall [24, 25], then traditional force control for gait recovery may not accommodate such a drastic dynamical shift in the interaction of the foot surface and the ground.

This paper builds on previous work using a 7 degree of freedom planar walking robot [2], in which we developed a stability region criterion for generating ZMP-based flat-footed walking on granular terrain, and applies the approach to the additional complexity of sloped granular terrain (Fig. 2, Section III). This work systematically varies gait parameters and experimentally assesses which adjustments yield effective gaits for planar locomotion on sandy slopes (Section IV). We generalize these effective gait parameters into a slope-dependent fitted function (in essence, a parameter lookup table) which results in ascending our experimental granular slope, shown in Fig. 1. Further, we perform a sensitivity study to show these generated gaits are robust to misestimation of the slope angle (Section IVC). For future work, this array of generated gaits can provide a baseline open loop scheme for higher-level feedback from inertial measurement units and force-sensing in the feet (Section VI).

II. BACKGROUND

A. Balancing of Bipeds on Flat Surfaces

Perhaps one of the most intuitive and widely implemented methods to balance a biped robotic system, and account for environmental disturbances, is through position and acceleration feedback, achieved by installing inertial measurement units (IMU's) at strategic points on the head or body of the system. Much like human reflexes, this sensory data is fed into a control center that then signals motion or repositioning of the torso or appendages as necessary. However [9], the idea of using this information to modify our open loop gait kinematics on granular material by taking advantage of the material properties of the substrate itself, has yet to be explored. This provides context for the experiments presented in this paper.

Typical bipedal walking has an alternating single and double support phase (SSP and DSP) [2], which is well studied for ground where a robot's feet do not have complex interactions, such as penetration or slip on the boundary of the surface. For biological systems, these complex surfaces are typically accounted for through sensing and processing of the resulting forces on the plantar surface of the foot, using input as a feed-forward into a complex, proprioceptive feedback system. In fact, it is difficult to enable and optimize walking in a robotic system over sand without estimation of the complex force interactions that occur at the surface [22, 23]; a phenomenon which was built upon in our previous work [2]. However, one of the key biological corrections that bipeds make using this force feedback is that of kinematic repositioning [26]. This supports the idea that adjusting the gait kinematics can allow slope climbing on complex terrain for biped robots. This was previously investigated for simulated human gait through variation of the parameters of step height, center of mass (CoM) height and step length

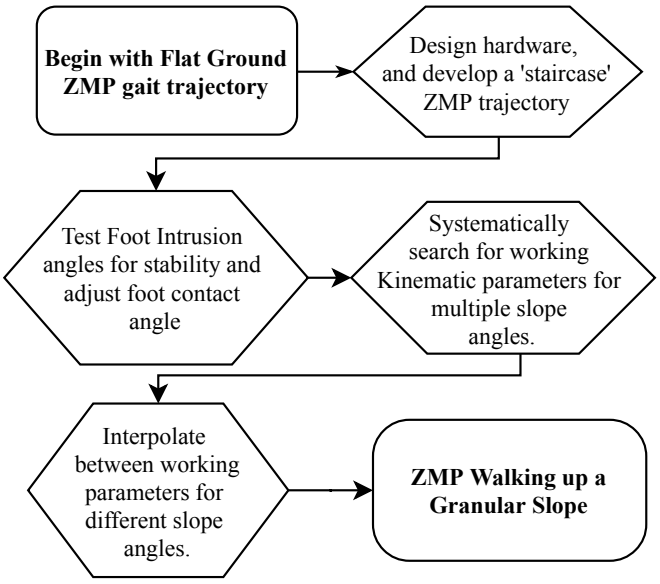

Fig. 2: A flow diagram outlining the experimental process for developing the ZMP gait design scheme that enables the planar biped walker to traverse a sandy slope.

[10]. These use simulated vestibular IMU input to control torso position, as well as a simulated kinesthetic sense through force and torque sensors to govern joint positions. The focus was a kinesthetic augmentation of the vestibular sense to provide stability when walking over complex terrain, and served as a good indicator of gait adjustments for uphill gait design.

B. Balancing of Bipeds on Staircases

in order to traverse a slope or inclined surface, the regular ZMP equation must be modified. This is because of the need to accommodate the fact that in any given phase where both feet make contact with the surface, one leg will be higher than the other [11]. Since traditional ZMP trajectories assume the contact point of both feet must be coplanar [11, 12], we considered the uphill trajectories of the robot to be along a virtual slope.

III. CONTROL AND EXPERIMENTAL METHODS

A. Walking on Flat Surfaces

ZMP Walking is based on the idea of the Linear Inverted Pendulum Model (LIPM) of bipedal walking, built upon the concept of a stability region in which stable gaits can be generated. One main characteristic of ZMP is that at any given moment, the trajectory of the gait places the biped within the stable region of the LIPM. Because the background work for ZMP walking assumes a constant vertical center of mass (CoM) height and constant foot position, for flat ground this position is determined using the following equations [1]:

$$P_{x-zmp} = \frac{-\tau_y}{mg} \tag{1}$$

$$P_{y-zmp} = \frac{\tau_y}{mg} \tag{2}$$

Where τ_x and τ_y are the torques on the ankle of the biped walker due to inertial effects of the biped, g is acceleration

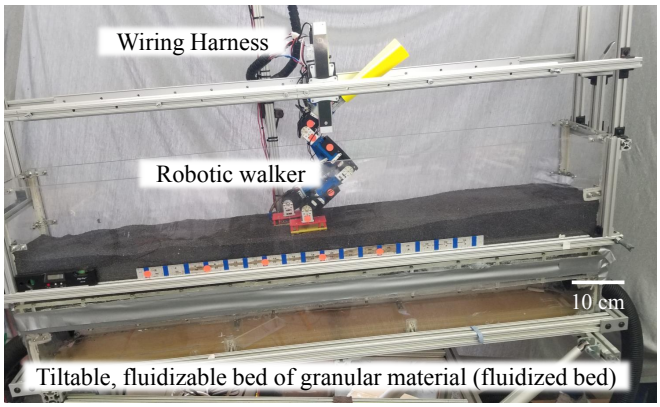

Fig. 3: Picture of the experimental setup showing placement of the walker on the bed. The sand bed that was used for testing constrains failure to a pitching axis, and can be set at angles between 0 and 25°. As stated, a specialized fluidizing bed was built that allows for uniform loose packing of the granular material that was used for our trials, in this instance poppy seeds. The robot was constructed using 6 Dynamixel MX-64A Servos and a 3D printed torso and leg links. A high torque torso servo was also used to support a counterweight which made up 0.23 kg of the 1.86 kg mass. Most of the heavy computing for the biped was done on a remote PC, connected through the wiring harness, with an small on-board micro-controller handling any intermediate processing of inertial and force feedback, and individual controllers on each servo governing position control of that particular motor.

due to gravity, and m is the robot mass. However, once we consider any deviation from walking on regular flat ground with constant center of mass, for instance, walking uphill on soft ground, we need to modify this equation in order to remain within a stability region. Since our biped system is constrained about the x-axis, this system can be simplified to:

$$P_{zmp} = P_{y-zmp} = \frac{\tau}{mg} \tag{3}$$

However, if we consider that the acceleration in the y - direction is given by:

$$\ddot{y} = \frac{g}{z}y - \frac{1}{mz}\tau_x \tag{4}$$

where z is the intersection distance from the contact point of the robot with the CoM plane. We can then use this information and substitute (2) into (4), resulting in:

$$P_{zmp} = P_{y-zmp} = y - \frac{z}{g}\ddot{y} \tag{5}$$

This is the governing equation for our planar ZMP walker, and the primary basis on which we begin to modify our gaits.

B. Zero Moment Point Walking on Sand - Stability Criterion Due to Sinkage and Slip

Our previous work demonstrated that the static placement of the foot allowed for the reactive terrain forces to balance the ankle torques. As such, the estimated stability region of the granular material needed to be equivalent to the stability region of the LIPM ZMP model. It is necessary to design trajectories such that that stability criterion is satisfied for all time [2] When we factor in the approximate sinkage of the granular matter to be traversed, we arrive at the model to calculate the trajectory of the robot joints T_{ZMP}, which can be given as a function, and is explored further in [2]:

$$T_{ZMP} = f(CoM, L, h, S, g, B_{front}, B_{back}) \tag{6}$$

Where CoM is the center of mass height, L is the biped step length, h is the step height, S is the sinkage of the biped, and B_{front} and B_{back} are the stability conditions of the biped for its given mass and size constraints.

To quantify our foot size, and thus B_{front} and B_{back} [2], we adapted the idea of the "polygon of stability" for locomotion on hard ground for use on granular media [2]:

$$d_c = \frac{L}{2}(1 - \frac{1}{\gamma}) \tag{7}$$

where we consider relationship of the planar foot length, L, to intrusion depth d_c and γ is the force overshoot ratio, which factors in force and velocity of the intrusion into the granular material, and can be obtained from literature [2].

C. Challenges of Walking on a Slope of Granular Terrain

Because the surface of the slope is that of granular material, a gait that addresses uphill climbing must be used with the same accommodations made for sinkage and equivalence of the stability regions. When designing our approach to this problem, the following were considered:

1) *Slippage and uniform compaction*: To provide a model of constant sinkage which could be estimated and eventually fed into a ZMP trajectory equation, it is necessary to have predictability of the behavior of the bed. A fluidized bed was built, as shown in Fig. 3, that allows for the repeatable preparation of uniform and loosely packed granular material, in this case poppy seeds [23]. Blowing air up through the base of the bed fluidizes the substrate when turned on, and after deactivating the blowers and letting the grains settle, a loosely packed and uniform granular surface remains. To accurately feed sinkage information into our ZMP trajectory generation algorithm, we first needed to know what the sinkage of the robot would be at a given weight. to address this, a simple measurement of parameters was conducted, as seen in Table 1. If the sinkage is not properly accounted for, we find that the robot gait will not compensate for the extra sink distance, and thus, the gait will fail and the robot will tip over.
2) *Failure of the substrate itself*: Another key challenge that we face when walking uphill on granular material is the failure of the surface itself, due to the effects

TABLE I: Robot and bed sinkage parameters for the 7 degree of freedom planar walker

Quantity	Value
Robot Mass	1.86 kg
Plantar Surface Area	100 cm3
Intrusion Depth	1.8 cm
Foot Length	20 cm
Foot Height	5 cm

of gravity, frictional forces, and lateral forces applied by the surface of the robot foot [24]. These complex interactions have been found to occur in slopes as low as 6° for the robot, and will be further discussed in Section V.

D. Developing a Staircase Gait

Staircase gaits have been studied with respect to ZMP trajectories for many years [11, 12]. Similarly, ZMP trajectories over uneven or complex terrain have also been very thoroughly explored, due to the fact that biped robots rarely operate in perfectly ideal situations [2, 10]. We seek to combine much of the work that has been done in order to allow for robust uphill walking uphill over granular material.

Because of inconsistencies in the ZMP trajectory formulation during the DSP of the walker, we use a virtual slope model [12]. Thus, we are left with an expression for stair climbing up a virtual slope that was implemented as our ZMP staircase equation [12]:

$$P_{zmp}\frac{k\ddot{y}+g}{g} = y - \frac{z}{g}\ddot{y} \tag{8}$$

This equation allows the trajectory of the foot to follow a staircase pattern, while allowing it's CoM to ascend the slope in a linear manner. However, implementation of a staircase gait by itself is not sufficient to implement on a slope with sinkage. Two major modifications were made to the trajectory generation to provide a novel, robust, and stable gait. Because the differences in slope angles are trigonometrically related to the "height of the stairs", the slope angle and intrusion angle of the foot were necessary augmentations of (6), such that the function to generate T_{ZMP} must include θ and ϕ as inputs:

$$T_{ZMP} = f(CoM, L, H, S, g, B_{front}, B_{back}, \theta, \phi) \tag{9}$$

Where θ is the slope angle of the sand,and ϕ is the intrusion angle of the foot, and $\phi/2$ the offset of the hip joints. Once this gait was developed, it was found that a traditional spline fit [2] of the ZMP trajectory path was sufficient only up to the point in the gait cycle that the robot seeks to compensate for sinkage (at the end of two full steps, or one full gait cycle). Because of this, a Savitsky Golay [15] criteria, or piecewise spline with history, was designed and used to generate a smoothed staircase trajectory for the robot to follow.

TABLE II: Joint trajectory generation for the planar walker

	Algorithm for Joint Trajectory generation
1)	Slope angle read in; L and CoM computed: $L,\ CoM = (\theta)$
2)	ZMP Trajectory Reference computed: $ZMP\ Ref = (s_{DSP0},\ s_{DSP},\ s_{SSP},\ n_{steps}, B_{front},\ B_{back},\ L)$
3)	ZMP Ref used to calculate CoM trajectory from Preview Control: $CoM\ Traj = (ZMP\ Ref,\ H,\ CoM,\ T,\ g,\ \theta)$
4)	CoM Traj used to plug into the robot inverse kinematics In general: $Q = (CoM\ Traj,\ backgoalposition,\ frontgoalposition)$ $Q_{initial} = (CoM\ Traj,\ 0,\ 0)$ $Q_{SSP1} = (CoM\ Traj,\ 0,\ sink+(L/2)tan(\theta))$ $Q_{DSP1} = (CoM\ Traj,\ 0,\ sink+(L/2)tan(\theta))$ $Q_{SSP2} = (CoM\ Traj,\ sink+(L/2)tan(\theta),\ sink+(L)tan(\theta))$ $Q_{DSP2} = (CoM\ Traj,\ sink+(L/2)tan(\theta),\ sink+(L)tan(\theta))$
5)	Repeat for n_{steps} if n_{steps} is complete: $Q_{SSPFinal} = (CoM\ Traj,\ sink+(L)tan(\theta),\ sink+(L)tan(\theta))$ $Q_{DSPFinal} = (CoM\ Traj,\ sink+(L)tan(\theta),\ sink+(L)tan(\theta))$
6)	Applying smoothing and adjustments: $Q_{intermediate} = (Q_{initial} + n_{steps}(Q_{SSP1}+Q_{DSP1}+Q_{SSP2}+Q_{DSP2})+Q_{SSPFinal}+Q_{DSPFinal})$ Q_{Final} = Savitsky-Golay($Q_{intermediate}$, ϕ)

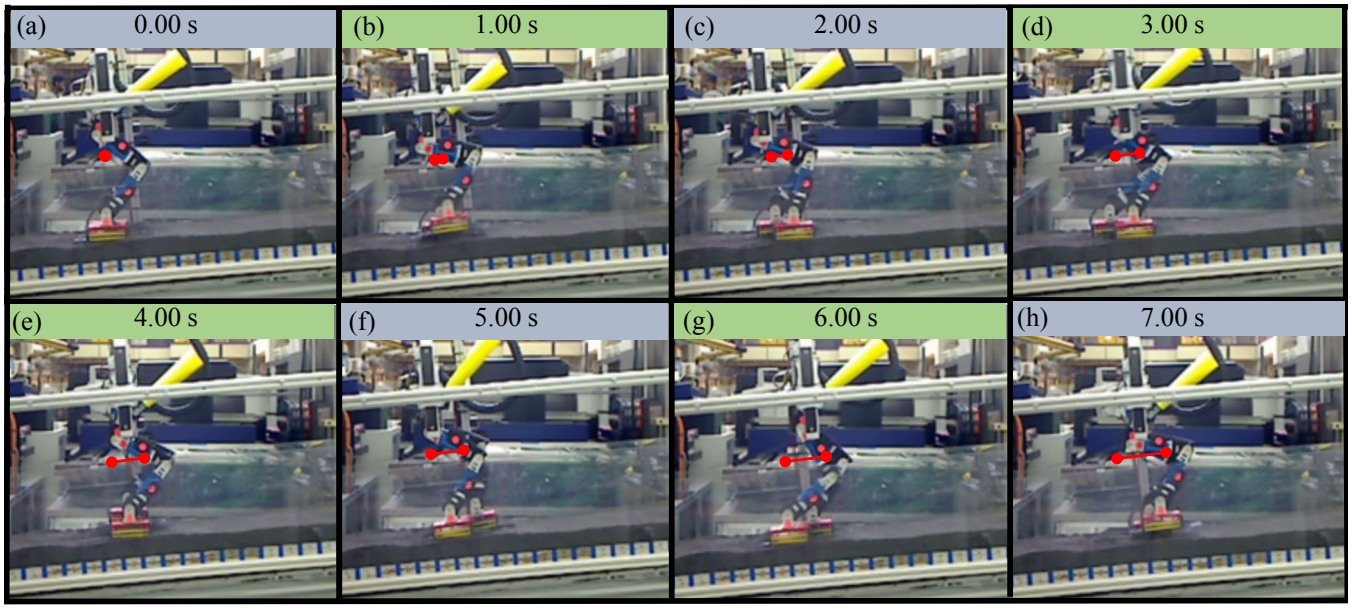

Fig. 4: Frame capture for the biped walker ascending a 4 degree incline. The robot begins ascending the slope by starting in the initial DSP (a), and continues to the first SSP (b), (c) until it arrives at the first intermediate DSP (d). From here, it switches feet, and the enters into the second SSP (e), (f), before arriving at the second DSP (g). The cycle then repeats (h) with the same SSP from (b), until the robot completes the commanded number of steps. From (a) to (h), the red line indicates the position of the center of mass at a given time. The true center of mass was used instead of the at the hip due to the low mass of the system.

E. Joint Angle Methods

Table 2 outlines the algorithm for the calculation of the joint trajectories. The process of Preview Control [1, 2, 11, 12] was used to generate ZMP references, which are then converted to joint angles through inverse kinematics. The necessary intrusion angle of the foot is represented by ϕ, and the forward hip posturing can be given as $\phi/2$. s_{DSP0} is the set number of initial double support samples, s_{DSP}, is the number of double support samples, s_{SSP} is the number of single support samples, n_{steps} is the number of steps, $Q_{initial}$ is the initial joint position matrix, Q_{SSP1} is the first SSP joint position matrix, Q_{DSP1} is the first DSP joint position matrix, Q_{SSP2} is the second SSP joint position matrix, Q_{DSP2} is the second DSP joint position matrix, $Q_{SSPFinal}$ is the final SSP joint position matrix, $Q_{DSPFinal}$ is the final DSP joint position matrix, $Q_{intermediate}$ is the pre-processed joint position matrix, Q_{final} is the final joint position matrix, and H is the preview horizon. An example of the implementation of this algorithm can be seen in Fig. 4.

IV. EXPERIMENTAL TRIALS AND RESULTS

A. Relation of Intrusion Angle and Sinkage to Slope Angle

We first sought to experimentally determine the ideal angle of foot intrusion for our system. From a systematic experimental sweep of foot angles, we found that the optimal foot angle was:

$$\theta = \phi. \tag{10}$$

The results of this experiment can be seen in Fig. 5, and was conducted as following:

1) *Establishing of Reference Frames*: The lab frame was used as reference, with the floor being 0°. The bed of poppy seeds was elevated to 5°.
2) *Sweep of Angles of Intrusion*: For N=5 trials for each slope angle, the walker was run for n= 4 steps, and a success was defined as the walker standing upright on two feet at the end of the trial, else a failure. This gave an experimental data set size of 96 total trials.

We hypothesize that a "placing" instead of a "digging" foot motion was more successful due to the relatively low mass and plantar pressure of the walker, compared to the "digging" behavior of humans which are significantly heavier [26].

B. Step Length, CoM and Angle Parameterization

Initially, the relationship in (8) was considered, and through systematic experimentation, a set of parameters (*CoM, L, H, S* and B_{front} and B_{back} being taken from our previous work) was identified that allowed for a stable gait at θ = 5°. The gait was then tested for a sweep of slope angles from θ = 0 to θ = 10 to test the general effectiveness of these parameters. The method used was:

1) Parameters that allowed for successful trials at θ=5 were used to generate a trajectories for n = 4 steps. A success was defined as the walker completing all 4 steps and returning to an initial DSP position. The bed was leveled and the ground was re-fluidized and reset before each trial.

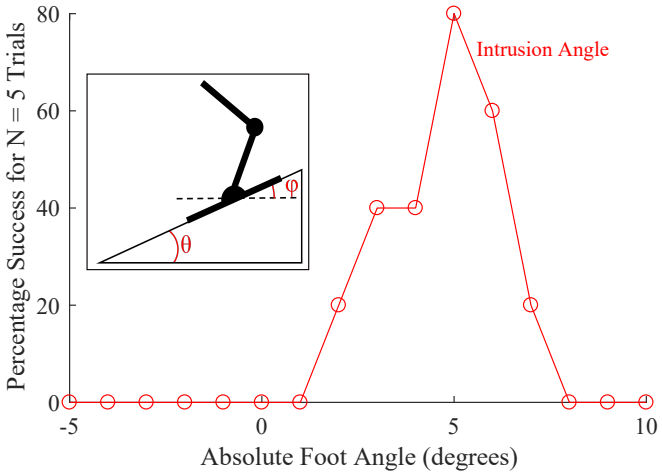

Fig. 5: Results of varying the intrusion angle of the foot on the slope surface where $\theta = 5$ is the slope angle, and ϕ is the absolute angle of the foot. Both θ and ϕ were measured in the lab frame. The highest rate of success was found to be tangent to the surface of the slope. We hypothesize that this is due to the low mass of the robot walker.

2) A sweep of trials from θ=0 to θ=10° with the modified staircase code was then run, with ϕ= θ and n= 10 trials. This gave an experimental control data set size of 100 total trials.
3) Failure modes were analyzed and processed. After this, through systematically incrementing and decrementing our values at each angle, a set of parameters *CoM, L, H* were also established for θ=0° to θ=10°, with a success being defined as the largest values of L and *CoM* to allow for at least 50% success for N = 10 gait trials at a given θ. This metric of success was chosen

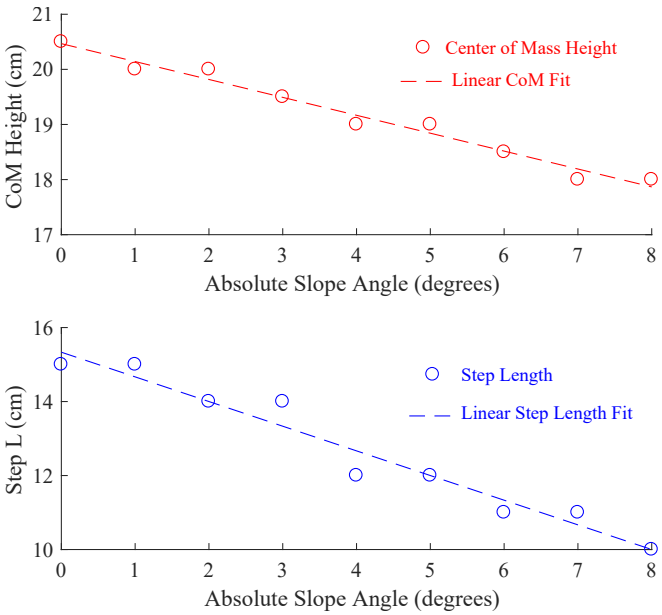

Fig. 6: Manually tuned gaits for specific slopes. These were then used to formulate a parameterized policy through the use of a linear fit. In (a), we see the results for Vertical CoM height, and in (b) we see the same experiment for step length. In order to accommodate increasing slope angles, we found that decreasing the Step Length and CoM height was necessary.

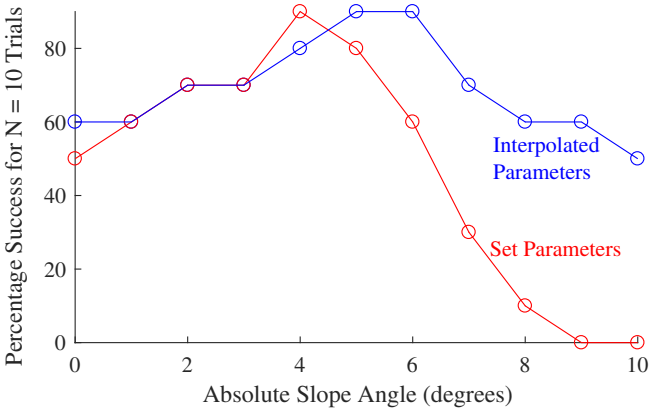

Fig. 7: Results of trials for set (L = 15cm, CoM = 20.5cm) and interpolated parameters using the staircase gait. When the same set parameters of L and CoM were used, there was a higher failure rate than when interpolated (connected) parameters were used. The similarity in the curves at angles lower than 6° is likely due to the fact that the gait was designed around a 5 degree incline, and then adapted to other slope angles accordingly.

due to the fact that we are primarily concerned with the locomotion of the robot on a granular incline, and as such, a larger L and CoM were favored.

4) The successful parameters from $\theta = 0^\circ$ to $\theta = 10^\circ$ were then fit with a linear regression, and equations that related all parameters to slope angle were identified for the planar walker. (Fig. 6).
5) Step 2) was then re-run, this time using the linear fit to select parameters. This gave an experimentally manipulated data set size of 100 total trials.

At this point, because the step length, CoM and step height were all related through a system of continuous linear equations, the robot had a specific gait for each slope angle within the limits of the hardware setup (angles of $0-10^\circ$, with a resolution of 0.01°). Once this parametrization was applied, we found that the robot was significantly more successful at traversing the sandy slope, due to the specificity of each gait to a particular incline. The results of this can be seen in Fig. 7. These results are encouraging, since we were able to improve our success rates at $\theta = 9^\circ$ and $\theta = 10^\circ$from 0% to 60% and 50% respectively; a substantial improvement over our initial trial.

C. Sensitivity Trials for Slope Angle

Once the gait was parameterized to be slope-specific, we tested the robustness of the parameterized gaits of the walker [27]. This served as a practical test of our method to misestimations of the slope angle. In order to do this, a second experiment was designed:

1) A slope angle of $\theta = 2^\circ$ was input into the gait code, for n = 6 steps. A success was defined as the walker completing all 6 steps and returning to an initial DSP position. The bed was leveled and the granular terrain was reset through the air fluidized before each trial.
2) The bed was raised to the θ input into the code, and the robot was run N = 3 times, each time recording the distance, and at the end of the third trial, establishing an average distance.
3) The bed was lowered to an angle of (θ–1°), while keeping an input angle of θ in the code, and the robot was run N = 3 times, each time recording the distance, and at the end of the third trial, establishing an average distance. This distance was then divided by the average distance at θ to obtain a relative distance traveled. This is important due to failure and slippage of the robot.
4) The bed was again lowered to (θ–2°) and the robot was run N = 3 times, each time recording the distance, and at the end of the third trial, establishing an average distance. This distance was once again divided by the distance traveled at slope θ in order to obtain a relative distance traveled. This process was further repeated at bed angles of ($\theta + 1^\circ$) and ($\theta + 2^\circ$).
5) The entire process was then repeated for θ=4°, 6°, 8° and 10°, giving a total of 150 experimental trials.

For low angles, ($\theta < 6^\circ$) we find that there is a reasonable level of robustness to perturbation in the open loop gait (Fig. 8). This is indicated by the high relative distances(fraction of distance covered at a particular offset angle, compared to the distance traveled when the slope angle is accurate to the gait) at lower inclines. However, at higher granular inclines, we observe large drop-off on either side of the sensitivity curve, once the gait is not specifically designed for that particular incline. It is this key fact that frames our current and future work.

V. DISCUSSION

A. Theoretical Basis For Experimental Success

As seen in 7 and 8, through the use of a simple linear fit, we were able to increase success rates from from 0% at $\theta = 9$ and $\theta = 10$ to 60% and 50% respectively. We theorize that this is due to the significant re-posturing of the 7- DOF system according to slope angle to remain within the polygon of stability. Similarly, this explains why the sensitivities drop off quite sharply at higher angles. If we consider that the support length normal to the lab frame is given by $Lcos(\theta)$ (5), we find that the polygon of stability becomes smaller as θ increases, thereby leading to more sensitive gaits.

B. Improving Sensitivity

As we examine the sensitivity curves, it becomes evident that the given scheme of gait generation is effective when the walker receives an accurate slope angle as input. However, for smaller perturbations, modeled as small offsets in slope angle from expected angle, we see that the gait effectiveness falls significantly – as much as 100% for 2 degree perturbations. Because of the nonlinear properties of granular material [24], we need to understand the force profiles at the foot-material boundary [23]. Unlike conventional balance control, to optimize biped walking over granular material it is necessary to characterize how the substrate itself actually yields. Once this is done, we hypothesize that through simple inertial control, for instance, in-the-loop torso repositioning, we can begin to improve sensitivity by combining the IMU

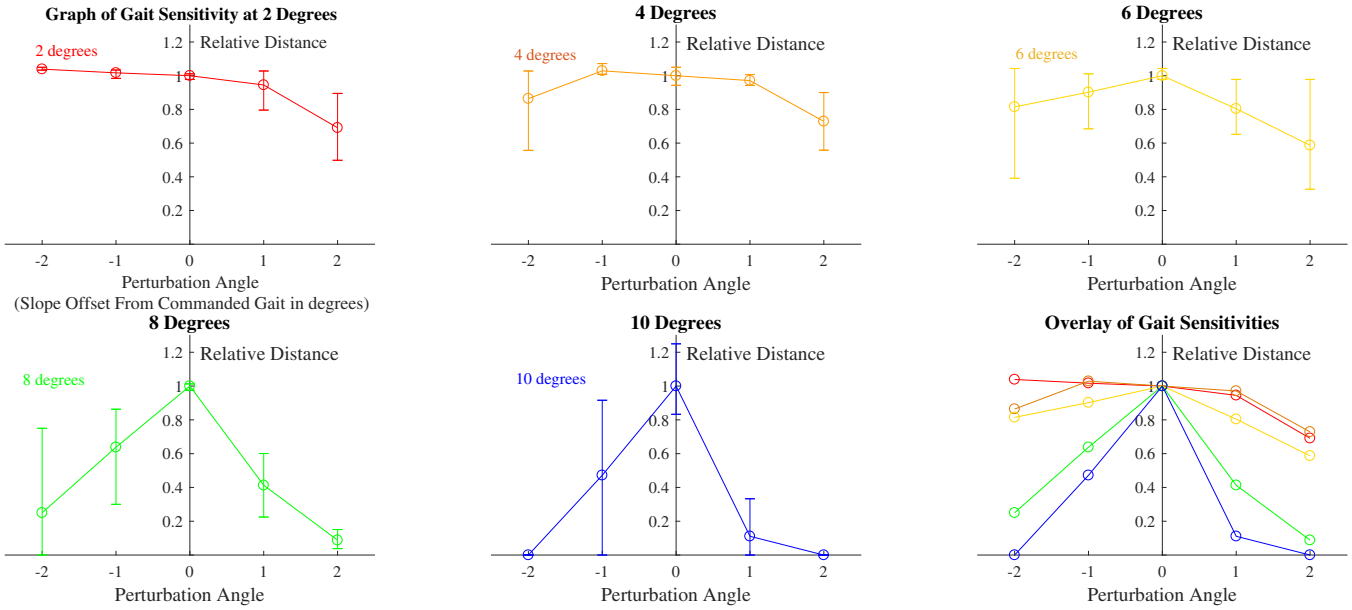

Fig. 8: Gait sensitivity plots for biped staircase ZMP gait from 2 to 10°. relative distance was used instead of absolute distance because of varying step lengths when climbing the slope. We see that as we deviate from the expected distance, we observe a significant decline in performance. This is especially apparent at steeper inclines. For a slope angle of 2°, the plan biped was still able to achieve a relative distance of over 0.6 for a perturbation of 2° in either direction. However, at 10°, this falls to 0.0.

and force feedback as a more biomimetic approach to biped walking on complex media.

C. Future Work

to expand upon the idea of using force profiles, future work will focus on using force sensing in the feet to inform real-time feedback control for the biped. We have installed both heel and toe force-moment sensors with the goal of detecting, in real time, if the gait is not progressing as planned. This force-based method of feedback also has the added advantage of distinguishing not only whether the machine is falling, but also the cause of the failure on complex terrain. Specifically, force feedback could be used to determine if the foot is slipping, avalanching the material, or hitting an unexpected bump, and then the robot adjust the joint kinematics accordingly in order to recover.

Another aspect that we are currently exploring is that the actual commanded distance does not always equate to traveled distance on a slope of granular material (Fig. 9). After inspection of videos of the foot-substrate interaction and flow, we hypothesize that this is due to slippage during the DSP, in which the robot is stable, but still slides incrementally backward as it positions its second foot. This is seen in Fig. 10.

VI. CONCLUSION

Through this study, we have examined the process of design, implementation and testing of a gait generation approach in which biped robots can be made to walk up a sandy slope. We introduced a robotic walking system and tested it using systematically determined parameters that successfully walked for a certain slope angle. We then related the kinematic parameters, particularly step length and CoM height, as an interpolated function of the slope angle itself, in order to traverse an uphill path of granular terrain. We found that the biped robot had the most success with the interpolated gait parameters being used as a result of sensing the slope angle. We further observed that as the slope intensity increases, the robustness of these gaits to perturbations significantly decreases. We hope to build upon these findings to improve the gait sensitivity through the use

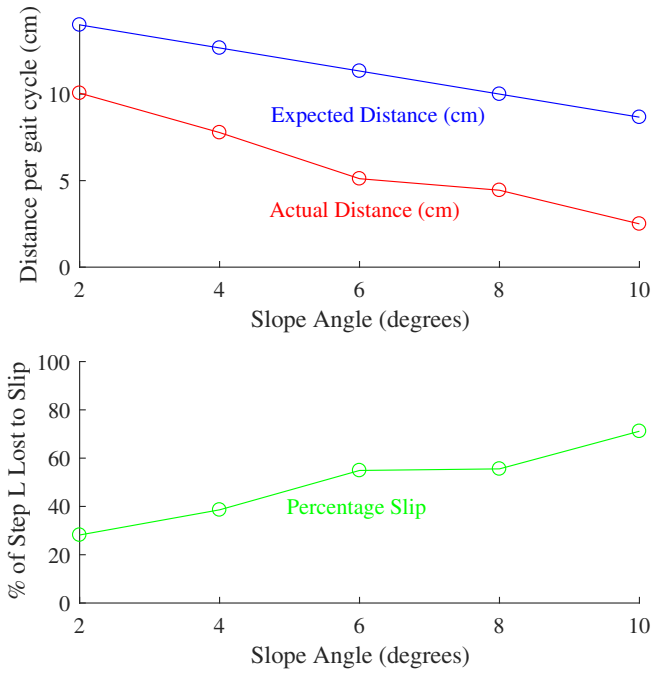

Fig. 9: Graph showing the actual and commanded distance for slope angles between 2° and 10°.This allows us to better understand and characterize the slipping (backward motion of the robot foot due to sliding on the granular surface) of the robot for each slope angle. As can be seen, the robot slips more as the slope becomes steeper

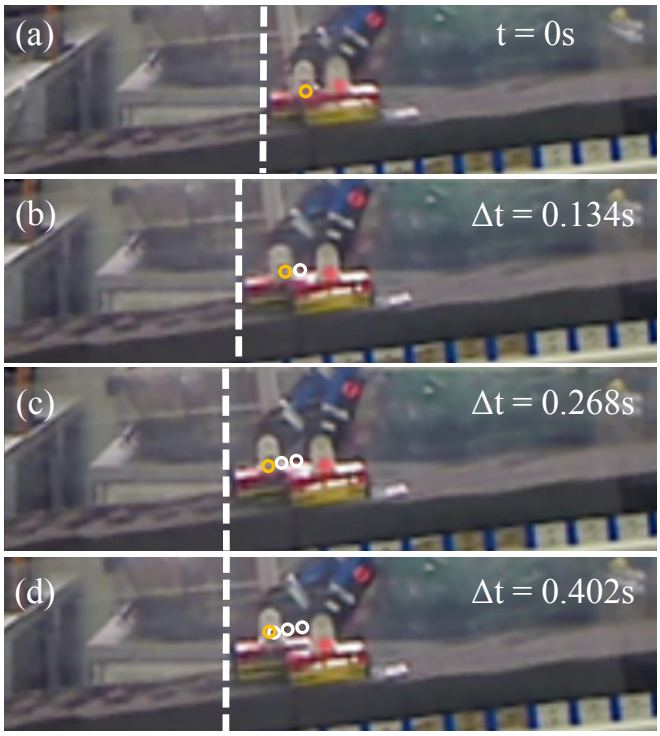

Fig. 10: A zoomed in profile of the foot slip during walking on a slope of granular material, where the dashed lines signify the back of the robot foot, the orange circles mark the current position of the ankle joint, and the white circles mark the cumulative positions for the displayed frames. In (a), the foot makes initial contact for a DSP with the sandy slope. In (b), the back foot begins to slide backward, instead of staying fixed on the ground as expected. in (c), the foot has arrived at its furthest position, and the robot begins another SSP as seen in (d).

of real-time feedback control and plantar force sensing.

APPENDIX

Supplementary footage for this experimental study may be found on the CRAB Lab Biped Walking Channel

ACKNOWLEDGMENT

We would like to thank all members of the Complex Rheology and Biomechanics (CRAB) Lab, particularly Yasemin Aydin for her technical advice, and Enes Aydin for his help in building the fluidized bed and the wiring harness setup.

REFERENCES

[1] S. Kajita, F. Kanehiro, K. Kaneko, K. Fujiwara, K. Harada, K. Yokoi, and H. Hirukawa, "Biped walking pattern generation by using preview control of zero-moment point," in *ICRA*, vol. 3, pp. 1620–1626, 2003.

[2] X. Xiong, A. D. Ames, and D. I. Goldman, "A stability region criterion for flat-footed bipedal walking on deformable granular terrain," in *Intelligent Robots and Systems (IROS), 2017 IEEE/RSJ International Conference on*, pp. 4552–4559, IEEE, 2017.

[3] E. R. Westervelt, J. W. Grizzle, and D. E. Koditschek, "Hybrid zero dynamics of planar biped walkers," 2003.

[4] A. D. Ames, "Human-inspired control of bipedal walking robots.," *IEEE Trans. Automat. Contr.*, vol. 59, no. 5, pp. 1115–1130, 2014.

[5] J. Pratt, J. Carff, S. Drakunov, and A. Goswami, "Capture point: A step toward humanoid push recovery," in *Humanoid Robots, 2006 6th IEEE-RAS International Conference on*, pp. 200–207, IEEE, 2006.

[6] A. Hereid, C. M. Hubicki, E. A. Cousineau, and A. D. Ames, "Dynamic humanoid locomotion: A scalable formulation for hzd gait optimization," *IEEE Transactions on Robotics*, 2018.

[7] C.-C. Huang, *Biped robot with a vestibular system*. PhD thesis, Virginia Tech, 1991.

[8] D. A. Winter, A. E. Patla, and J. S. Frank, "Assessment of balance control in humans," *Med Prog Technol*, vol. 16, no. 1-2, pp. 31–51, 1990.

[9] A. V. Cuppone, V. Squeri, M. Semprini, L. Masia, and J. Konczak, "Robot-assisted proprioceptive training with added vibro-tactile feedback enhances somatosensory and motor performance," *PloS one*, vol. 11, no. 10, p. e0164511, 2016.

[10] K. Hashimoto, Y. Takezaki, H. Motohashi, T. Otani, T. Kishi, H.-o. Lim, and A. Takanishi, "Biped walking stabilization based on gait analysis," in *Robotics and Automation (ICRA), 2012 IEEE International Conference on*, pp. 154–159, IEEE, 2012.

[11] W. Huang, C.-M. Chew, Y. Zheng, and G.-S. Hong, "Pattern generation for bipedal walking on slopes and stairs," in *Humanoid Robots, 2008. Humanoids 2008. 8th IEEE-RAS International Conference on*, pp. 205–210, IEEE, 2008.

[12] T. Sato, S. Sakaino, E. Ohashi, and K. Ohnishi, "Walking trajectory planning on stairs using virtual slope for biped robots," *IEEE transactions on industrial electronics*, vol. 58, no. 4, pp. 1385–1396, 2011.

[13] K. Kondak and G. Hommel, "Control algorithm for stable walking of biped robots," in *Proceedings of the International Conference on Climbing and Walking Robots (CLAWAR)*, pp. 119–126, 2003.

[14] A. Hereid, S. Kolathaya, M. S. Jones, J. Van Why, J. W. Hurst, and A. D. Ames, "Dynamic multi-domain bipedal walking with atrias through slip based human-inspired control," in *Proceedings of the 17th international conference on Hybrid systems: computation and control*, pp. 263–272, ACM, 2014.

[15] A. Polanski, A. Switonski, H. Josinski, K. Jedrasiak, and K. Wojciechowski, "Estimation system for forces and torques in a biped motion," in *International Conference on Computer Vision and Graphics*, pp. 185–192, Springer, 2010.

[16] Q. Huang, Y. Nakamura, and T. Inamura, "Humanoids walk with feedforward dynamic pattern and feedback sensory reflection," in *Robotics and Automation, 2001. Proceedings 2001 ICRA. IEEE International Conference on*, vol. 4, pp. 4220–4225, IEEE, 2001.

[17] P. F. Meyer, L. I. Oddsson, and C. J. De Luca, "The role of plantar cutaneous sensation in unperturbed stance," *Experimental brain research*, vol. 156, no. 4, pp. 505–512, 2004.

[18] Y. Wang and S. Wang, "A new directional-intent recognition method for walking training using an omnidirectional robot," *Journal of Intelligent & Robotic Systems*, vol. 87, no. 2, pp. 231–246, 2017.

[19] P.-B. Wieber, "Trajectory free linear model predictive control for stable walking in the presence of strong perturbations," in *IEEE-RAS international conference on humanoid robots*, 2006.

[20] C. G. Atkeson and B. Stephens, "Multiple balance strategies from one optimization criterion," in *Humanoid Robots, 2007 7th IEEE-RAS International Conference on*, pp. 57–64, IEEE, 2007.

[21] M. Morisawa, S. Kajita, F. Kanehiro, K. Kaneko, K. Miura, and K. Yokoi, "Balance control based on capture point error compensation for biped walking on uneven terrain," in *Humanoid Robots (Humanoids), 2012 12th IEEE-RAS International Conference on*, pp. 734–740, IEEE, 2012.

[22] J. Aguilar, T. Zhang, F. Qian, M. Kingsbury, B. McInroe, N. Mazouchova, C. Li, R. Maladen, C. Gong, M. Travers, *et al.*, "A review on locomotion robophysics: the study of movement at the intersection of robotics, soft matter and dynamical systems," *Reports on Progress in Physics*, vol. 79, no. 11, p. 110001, 2016.

[23] C. Li, T. Zhang, and D. I. Goldman, "A terradynamics of legged locomotion on granular media," *Science*, vol. 339, no. 6126, pp. 1408–1412, 2013.

[24] N. Gravish and D. I. Goldman, "Effect of volume fraction on granular avalanche dynamics," *Physical Review E*, vol. 90, no. 3, p. 032202, 2014.

[25] B. McInroe, H. C. Astley, C. Gong, S. M. Kawano, P. E. Schiebel, J. M. Rieser, H. Choset, R. W. Blob, and D. I. Goldman, "Tail use improves performance on soft substrates in models of early vertebrate land locomotors," *Science*, vol. 353, no. 6295, pp. 154–158, 2016.

[26] T. M. Lejeune, P. A. Willems, and N. C. Heglund, "Mechanics and energetics of human locomotion on sand.," *Journal of Experimental Biology*, vol. 201, no. 13, pp. 2071–2080, 1998.

[27] H. Marvi, C. Gong, N. Gravish, H. Astley, M. Travers, R. L. Hatton, J. R. Mendelson, H. Choset, D. L. Hu, and D. I. Goldman, "Sidewinding with minimal slip: Snake and robot ascent of sandy slopes," *Science*, vol. 346, no. 6206, pp. 224–229, 2014.